The *SLT2 (MPK1)* MAP Kinase Homolog Is Involved in Polarized Cell Growth in *Saccharomyces cerevisiae*

Cristina Mazzoni, Patrick Zarzov, Alain Rambourg,* and Carl Mann

Service de Biochimie et Génétique Moléculaire, *Service de Biologie Cellulaire, Centre d'Etudes de Saclay, 91191 Gif-sur-Yvette, France

Abstract. Bud emergence, spindle pole body duplication and DNA replication are all dependent on the activation of the *CDC28* protein kinase at the Start point in the G1 phase of the cell cycle. Bud emergence requires polarization of the cytoskeleton and secretory vesicles to a specific site on the cell surface. Cdc28p activated by G1-cyclins triggers polarization of actin to the site of bud emergence and favors apical bud growth (Lew, D. J., and S. I. Reed. 1993. *J. Cell Biol.* 120:1305-1320). We isolated *slt2-1* as a mutation that enhances the division defect of *cdc28* mutants with defects at Start. Slt2p(Mpklp) is a member of the MAP kinase family (Lee, K. S., K. Irie, Y. Gotoh, Y. Watanabe, H. Araki, E. Nishida, K. Matsumoto, and D. E. Levin. 1993. *Mol. Cell. Biol.* 13:3067-3075). We show that *slt2* mutants exhibit phenotypes similar to those shown by mutants of the yeast actin cytoskeleton, including delocalization of chitin deposition and of actin cortical spots and the accumulation of secretory pathway membranes and vesicles. Furthermore, *slt2::HIS3 act1-1* and *slt2::HIS3 myo2-66* double mutants are inviable. We suggest that Slt2p functions downstream or in parallel with Cdc28p in promoting bud formation and apical growth.

CELL reproduction involves cell cycle-specific events occurring both in the nucleus and in the cytoplasm. In the budding cell cycle of *Saccharomyces cerevisiae*, a number of stage-specific events direct the position and the morphology of the bud. These events include the choice of a bud site, the localization of a specific group of proteins to the site from which the bud will emerge, and the polarization of cell surface growth to the new bud site. Assembly of the bud-site complex is required for the polarization of the yeast cytoskeleton and the targeting of secretory vesicles to the bud site (for reviews see references 9, 12, 32).

The initial growth of the bud is highly polarized. Actin cortical patches (22), calmodulin (6), and the *SPA2* protein (53, 54) are localized to the tips of the bud during this period of apical growth. Actin localization and bud growth are less polarized later in the cell cycle. The timing of this shift and the degree of delocalization determine bud shape, with isotropic growth favoring spherical forms (28, 55).

The entry into a new cell cycle involves the coordinated but independent pathways of bud initiation, spindle pole body duplication, and nuclear DNA synthesis (43). The triggering of these pathways all require the activation of the *CDC28* protein kinase in the G1 phase of the cell cycle (45). This regulatory point of the cell cycle has been baptized "Start" (18). The manner in which the *CDC28* kinase promotes bud formation at Start is not well defined. Lew and Reed (28) have shown that actin polarization can be triggered by the kinase activity of Cdc28p complexed with G1 cyclins, and they mapped the time at which actin polarization occurs in their synchronized cells to be soon after Start. Localization of Cdc3p (23) and Spa2p (54) to the presumptive bud site occurs substantially before bud emergence, but the precise timing of these events relative to *CDC28* kinase activation at Start was not examined. However, *cdc28* mutants at their restrictive temperature and wild-type cells treated with mating pheromone can polarize their growth to form a projection in the apparent absence of *CDC28* kinase activity (28, 31, 54). These observations suggest that a pathway for polarizing growth independent of Cdc28p also exists in *S. cerevisiae.*

We isolated a mutation of the *SLT2(MPK1)* MAP kinase gene that augments the division defect of cells expressing a partially inactivated *cdc28* mutant. We show that *slt2* mutants exhibit defects in cell polarity and accumulate secretory vesicles. We suggest that Slt2p acts downstream or in parallel with Cdc28p to promote bud morphogenesis.

Materials and Methods

Yeast Strains and General Methods

The yeast strains used in this study are listed in Table I. The *cdc28-109* allele was found amongst a collection of *cdc28* mutants in the Department of Genetics (University of Washington, Seattle, WA). Its characterization will

Address all correspondence to Carl Mann, SBGM, Bât 142, Centre d'Etudes de Saclay, F-91191 Gif-sur-Yvette, France.

Dr. Mazzoni's present address is Dipartimento di Biologia Cellulare e dello Sviluppo, Università di Roma "La Sapienza," Città Universitaria, Piazzale Aldo Moro, 00185 Roma, Italia.

be described elsewhere. The CML6 and CML13 *SLT2*$^+$ strains were obtained by transforming respectively CMY678 *MATα slt2-1* and CML12 *MATa slt2-1* strains with a YIp-*URA3-SLT2* plasmid and targeting plasmid integration to the *slt2-1* site. *SLT2*$^+$ *ura3*$^-$ segregants were then selected by growth on a 5-fluoro-orotic acid (FOA)[1]-containing medium. Media containing FOA for the counterselection of *URA3*$^+$ plamids were prepared as described (3). Standard genetic and molecular manipulations were performed as described (49, 50). The segregation in genetic crosses of *cdc28-109*, *slt2*, *act1*, and *myo2-66* was followed by complementation testing of the temperature-sensitive mutations.

Determination of Cell Volumes

Cell volumes were determined by photographing cells at 250× magnification with a Zeiss Axioplan light microscope equipped with differential interference contrast optics. The negatives were projected onto a flat surface and the major and minor axes of unbudded cells and the mother cell portions of budded cells were measured. Cell volumes were estimated by assuming the cells to be prolate ellipsoids and using the formula $V = 4\pi ab^2/3$, where a is the semi-major axis and b is the semi-minor axis. At least 250 cells were measured for each population examined.

Time Lapse Photomicroscopy

5 μl of a cell suspension containing approximately 6×10^6 cells per ml were placed on a thin layer of YPD agar on a microscope slide. A cover slip was placed over the cells and cell proliferation was followed by differerential interference contrast microscopy at a magnification of 250×.

Fluorescence Microscopy

Cells were fixed in 3.7% formaldehyde and stained with Calcofluor to detect chitin or with rhodamine-conjugated phalloidin to detect filamentous actin as described (42, 44), except that rhodamine-phalloidin (Sigma Immunochemicals, St. Louis, MO) was dissolved in phosphate-buffered saline at 100 mM and used at a final concentration of 6.6 mM.

Cloning and Disruption of SLT2

The temperature-sensitive mutation in strain CMY678 was isolated as being colethal with *cdc28-109* at 28°C (see Results). CMY678 was transformed with DNA libraries constructed in the centromeric plasmid YCp50 (47) and in the multicopy vector pFL44 (4) and temperature-resistant Ura$^+$ transformants were selected at 37°C. One plasmid from the YCp50 bank and several plasmids from the pFL44 bank were found that restored wild-type growth to the mutant. Restriction enzyme analysis of these plasmids showed them all to contain genomic DNA inserts derived from the same chromosomal region. A *URA3* plasmid integrated at this chromosomal locus was found to be tightly linked to the *slt2-1* mutation in CMY678 by tetrad analysis (no recombination between *URA3* and *slt2-1* in 10 complete tetrads), thereby demonstrating that we had cloned the corresponding wild-type gene. A 2.2-kb KpnI/BglII restriction fragment from this region was able to complement the CMY678 temperature-sensitive phenotype when cloned into the centromeric vector pRS316 (51). An open reading frame on this fragment was necessary for the complementation and its DNA sequence showed it to be identical to the previously described *SLT2* gene (60), except for three nucleotide differences. In the numbering scheme of Fig. 3 of Torres et al. (60), we found C at nucleotide 1035 in place of G, leading to the substitution of valine at amino acid 126 for leucine, and we found CG at nucleotide positions 2270 and 2271 instead of GC, leading to the substitution of threonine at amino acid 467 in place of serine. After determining the identity of the gene, we named our EMS-induced mutation *slt2-1*.

An *slt2::HIS3* disruption was made by substituting a 1.3-kb HindIII fragment internal to the *SLT2* gene carried on pRS316 with a 1.7-kb *HIS3* fragment. The resulting construction deletes all but the first 219 bp of *SLT2* coding sequence. Digestion of the pRS316-*slt2::HIS3* plasmid with EcoRI +XbaI releases a fragment of about 2.3 kb that may be used to disrupt the *SLT2* gene by one-step gene replacement (48).

Electron Microscopy

Yeast cells were fixed by addition of glutaraldehyde directly to the YPD growth medium at a final concentration of 2% (vol/vol) for ~30 min. Cells were then centrifuged, resuspended in a buffer containing 2% glutaraldehyde, 0.1 M sodium cacodylate (pH 7.4), and 0.8 M sorbitol, and then incubated overnight. Cells were then postfixed for 1 h in reduced osmium (a 1:1 mixture of 2% aqueous osmium tetroxide and 3% aqueous potassium ferrocyanide), dehydrated in ethanol, and embedded in Epon. 80-nm sections were cut with a Reichert ultramicrotome, stained for 2 min with lead citrate and examined at 80 kV with a Philips CM12 electron microscope.

Results

Isolation of slt2-1^{ts} As a cdc28-colethal Mutation

In the hope of identifying functions that are required either downstream or in parallel with the *CDC28* protein kinase for cell-cycle progression, we are isolating mutants that are colethal (synthetically lethal) with *cdc28*. A *cdc28*-colethal mutant is one which in combination with a temperature-sensitive *cdc28* mutant prevents growth at a normally per-

1. *Abbreviation used in this paper*: FOA, 5-fluoro-orotic acid.

Table I. Yeast Strains Used in This Study

Name	Genotype	Source
CMY678	*Matα, slt2-1, ura3-52, leu2, trp1, ade2, lys2-801*	
CML6	CMY678 *SLT2*$^+$ isogenic strain	This study
CML12	*Mata, slt2-1, ura3-52, trp1, ade2, lys2-801, leu2*	This study
CML13	CML12 *SLT2*$^+$ isogenic strain	This study
CML14	*Matα, slt2-1, ura3-52, trp1, ade2, lys2-801, his3Δ200*	This study
CML15	*Mata/α, slt2-1/slt2-1, ura3-52/ura3-52, trp1/trp1, ade2/ade2, lys2-801/lys2-801, leu2/LEU2 his3Δ200/HIS3*	This study
SC55	*Mata/α, ura3-52/ura3-52, trp1Δ1/trp1Δ1, his3Δ200/his3Δ200, ade2-101/ade2-101, lys2-801/lys2-801, leu2/LEU2 can^r/CAN^s*	This study
CML20	*Mata, slt2Δ::HIS3, ura3-52, trp1Δ1, ade2-101, lys2-801*	This study
CML22	*Mata, ura3-52, trp1Δ1, his3Δ200, ade2-101, lys2-801*	This study
CMY712	*Mata, cdc28-4, ura3-52, trp1Δ1, leu2Δ1, his3Δ200, ade2-101, tyr1*	This study
CML27	*Matα, slt2Δ::HIS3, ura3-52, trp1Δ1, ade2-101, leu2Δ1*	This study
CML29	*Mata, slt2Δ::HIS3, ura3-52, trp1Δ1, ade2-101, (leu2Δ1, lys2-801 ?)*	This study
CMY776	*Matα, act1-1, ura3-52*	Novick and Botstein, 1985 and this study
CMY830	*Mata, myo2-66, ura3-52, leu2Δ1, ade2-101, his3Δ200, his6*	Johnston et al., 1991 and this study
YC190	*Mata, ura3-52, lys2-801, ade2-101, his3Δ200, trp1Δ1, leu2Δ90, slk1Δ1::TRP1*	Costigan et al., 1991
CMY715	*Mata, cdc28-1N, ura3-52, leu2Δ1, lys2-801*	This study

missive temperature for either single mutant. A conceptually similar scheme was used to search for possible downstream effectors of the *Drosophila sevenless* protein kinase (52). The results of this screen will be described in detail elsewhere. Briefly, a *cdc28-109* temperature-sensitive mutant was transformed with an autonomously replicating plasmid containing the *URA3* and *CDC28* genes (YEp24-*CDC28*). These cells were then mutagenized with ethylmethanesulfonate and spread on YPD plates to have individual colonies at the permissive temperature (24°C) for the *cdc28-109* mutant. The colonies were then replicated at the semi-permissive temperature of 28°C to plates containing media either selecting for (synthetic medium without uracil [-Ura]) or counterselecting (synthetic medium containing FOA) the YEp24-*CDC28* plasmid. Colonies able to grow on the -Ura plates but not the FOA plates at 28°C were considered to harbor mutations colethal with *cdc28-109*. We next screened amongst the colethal mutations for those that caused temperature-sensitive growth at 37°C even in the presence of a wild-type *CDC28* gene. One such mutation, *slt2-1* (see below), was seen to give rise to a population of unusually small cells at the restrictive temperature and is the subject of this paper. The *cdc28-109 slt2-1*/YEp24-*CDC28* mutant strain was backcrossed to a wild-type strain and tetrads were dissected after sporulation of the resulting diploid strain. The traits of colethality with *cdc28-109* at 28°C and temperature sensitivity for growth at 37°C were linked and segregated as a single mutation in 12 tetrads.

The *cdc28-109* mutation leads to an arrest of cell division in both the G1 and G2 phases at the restrictive temperature of 37°C (unpublished data). To see if the incompatability between the *slt2* and *cdc28* mutations could be assigned to a G1 or G2 specific function of *cdc28*, we crossed the *slt2-1* mutant with *cdc28-4* and *cdc28-1N* mutants. The *cdc28-4* mutation preferentially inactivates the G1 function of Cdc28p (46), whereas the *cdc28-1N* allele preferentially inactivates a G2/mitotic function of the kinase (40, 57). *slt2-1 cdc28-1N* double mutants were readily obtained and grew as well as the individual single mutants at the permissive temperature for these mutants. In contrast, the *slt2-1 cdc28-4* double mutants, although viable at 24°C, grew more slowly and exhibited phenotypes at 24°C that were only seen at higher temperatures in the single mutants. Furthermore, *cdc28-4* and *slt2-1* mutants can each grow at the semi-permissive temperature of 30°C, whereas the double mutant was inviable at this temperature. These genetic interactions suggest that *CDC28* and *SLT2* cooperate in performing a G1-specific function.

A DNA fragment complementing the *slt2-1* temperature-sensitive growth defect was obtained from a YCp50 yeast genomic DNA library (47). DNA sequencing of the complementing region revealed the presence of a gene identical to the previously described *SLT2* (suppressor of *lyt2*) gene (60), except for three nucleotide differences (see Materials and Methods). The *SLT2* gene encodes a protein that is similar to the *CDC28*, *FUS3*, and *KSS1* protein kinases (26, 60). Cdc28p is a member of the CDC2 family of protein kinases whereas Fus3p and Kss1p are members of the MAP/ERK family of kinases. A sequence comparison of Slt2p with all known CDC2-like and MAP kinases shows that Slt2p clearly belongs to the MAP kinase family (Fig. 1). Slt2p has a carboxy-terminal extension relative to most of the CDC2/CDC28 and MAP kinases. If only the shared catalytic domains are considered, Slt2p is about 28% identical to the CDC2/CDC28 kinases compared to about 42% identity with the MAP kinases. The sequence PSTAIRE is present in most of the CDC2-like kinases and has been implicated in the binding of mitotic cyclins (13). The PSTA portion of PSTAIRE is not conserved in SLT2 (aa 66-72) and the MAP kinases. The sequence GTYG is present near the aminoterminus of all the CDC2/CDC28 kinases. An inhibitory phosphorylation of this tyrosine residue, and sometimes the adjacent threonine residue, regulates the timing of activation of CDC2 and the entry into mitosis (37). In SLT2 (amino acids 32–35) and the MAP kinases, this sequence is replaced by GAYG and there is no evidence so far for the phosphorylation of the tyrosine residue in this sequence. Furthermore, we have identified an additional 8-amino acid residues (Fig. 1) that are conserved in all MAP kinase homologs examined to date, including SLT2, but are not found in any of the *CDC2*-like kinases. Amongst these is a tyrosine residue (aa 192 of SLT2) whose phosphorylation by distinct MAP kinase kinases is required for the activation of the MAP kinases (24). This tyrosine residue is contained within the sequence TEY found in all MAP kinases except the recently identified HOG1 kinase (5), where it is TGY. The *SLT2* gene has also been re-isolated by Lee et al. as a multicopy suppressor of a *bck1(slk1)* mutant (26). They have shown that a *Xenopus* MAP kinase can complement an *slt2* mutation, that mutation of threonine-190 to alanine or tyrosine-192 to phenylalanine inactivates SLT2, and they have renamed the gene *MPK1*.

A multicopy plasmid containing an *SLT2* gene deleted for the sequence encoding the last 158 amino acids of the protein was obtained while isolating multicopy suppressors of a *cdc28-1N* mutation (Marc Blondel, personal communication). This deletion removes the carboxy-terminal amino acid sequence specific to *slt2p* as well as two residues (glu327 and pro328) that are found in all MAP kinases examined to date (see Fig. 1). Further examination showed that this plasmid could partially suppress the temperature-sensitive phenotype of the *cdc28-1N* mutation, but was incapable of complementing the *slt2-1* mutation. The *cdc28-1N* allele gives a G2/mitosis-specific arrest at 37°C (40, 57). We found that both the truncated *SLT2* gene and the intact *SLT2* gene on multicopy plasmids were capable of partially suppressing the *cdc28-1N* temperature-sensitive phenotype. We interpret these results as indicating that the *slt2p* truncation deletes residues that are required for the function of *slt2p*, but not necessarily for the basic kinase activity of the protein. In this model, the partial suppression of the *cdc28-1N* mutation might be explained by the ability of the overexpressed *SLT2* kinase, in its intact or truncated form, to phosphorylate certain critical substrates of *CDC28* in G2/mitosis. This possibility is rendered plausible by the similarity in structure and substrate specificity of the CDC2 and MAP kinase families (39). Wild-type cells are transiently inhibited in their growth after transformation with multicopy plasmids containing the intact or truncated *SLT2* gene, but then seem to adapt to this overexpression and grow normally.

Phenotypic Characterization of the slt2-1 Mutant

Disruption of the *SLT2 (MPK1)* gene caused a temperature-sensitive cell lysis phenotype (26, 60). We observed a similar

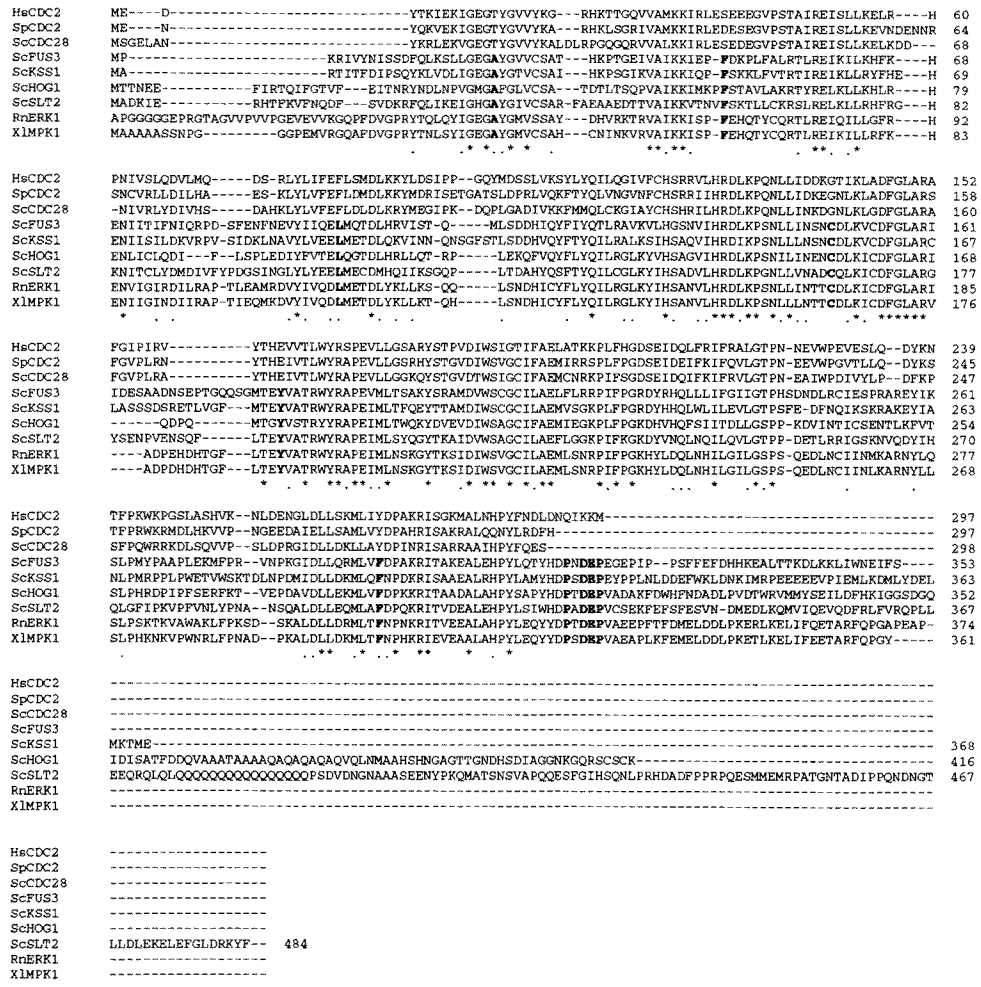

Figure 1. Sequence comparison of SLT2 with representative members of the MAP kinase and CDC2/CDC28 kinase families showing SLT2 to belong to the MAP kinase family. Residues that are absolutely conserved amongst MAP kinase family members (including SLT2), but not found in the CDC2/CDC28 kinases are highlighted in bold. This comparison was based on an examination of 15 MAP kinase sequences and 13 CDC2/CDC28/CDK2 kinase sequences found in the sequence databases, but only a representative sample is shown here in order to conserve space. Asterisks indicate residues that are identical between the MAP and CDC2/CDC28 kinases and dots indicate evolutionarily conserved residue substitutions for the MAP and CDC2/CDC28 kinases. The sequences shown are CDC2 from *Homo sapiens* and *Schizosaccharomyces pombe* and CDC28 from *S. cerevisiae*. Representatives of the MAP kinase family include: FUS3, KSS1, HOG1 and SLT2 from *S. cerevisiae*, ERK1 of *Rattus norvegicus* and MPK1 of *X. laevis*.

phenotype for the EMS-induced *slt2-1* mutation. Transfer of *slt2-1* cells from 24° to 37°C leads to a rapid loss of cell viability (Fig. 2 *A*) associated with a large degree of cell lysis as seen by phase contrast microscopy. The cell division arrest was not homogeneous, although the percentage of unbudded cells increased at 37°C from 49 to 71% before death of most cells in the culture after 4 h of incubation. A proportional increase in the fraction of cells with a G1 DNA content was observed at 37°C as monitored by cytofluorimetry (data not shown). Cell lysis was observed for both budded and unbudded cells in the culture.

We additionally noticed a novel *slt2* phenotype: mutant cells exhibit a strikingly heterogeneous range of sizes including unusually small cells with a characteristic pear-shaped morphology and abnormally large, round cells. This size heterogeneity was characterized by measuring cell volumes from photomicrographs. At the permissive temperature of 24°C, exponentially growing *slt2-1* cells were highly viable with little or no signs of cell lysis, but a subpopulation of small cells was manifest that was never seen in the wild-type control strain (Fig. 2, *B* and *C*). Transferring the cells to the semi-permissive temperature of 30°C increased dramatically the cell size heterogeneity and increased the percentage of unbudded cells in the population from 49 to 66%. After 4 h at 30°C, about 20% of the cells were unusually small. At the same time, a subpopulation of unusually large, round cells was observed. Although the *slt2-1* cells can be grown continuously at 30°C, there is a significant level of cell death observed at this temperature (Fig. 2 *A*). Transferring cells from 24° to 37°C also induced a cell size heterogeneity (Fig. 2, *B* and *C*) that was accompanied at this temperature by the death of the entire population (Fig. 2 *A*). An isogenic *SLT2* strain showed no change in its cell-size distribution when transferred from 24° to 30°C. Transferring the *SLT2* strain from 24° to 37°C for 4 h caused an overall shift to larger cell sizes compared to 24°C (Fig. 2 *C*) that may be attributed to a transitory G1 arrest associated with the 37°C heat shock (21). Note, however, that the cell size distribution remains clustered and no small cells are generated.

We never observed a bud associated with the subpopulation of small, pear-shaped *slt2* cells. Time-lapse photomicrography (Fig. 3) demonstrated that these cells were in fact stillborn. The small cells are stillborn even at the permissive temperature of 24°C where the vast majority of *slt2-1* cells are viable (Fig. 2 *A*). We do not know why these cells are dead. Staining of DNA with the fluorochrome DAPI showed that the small, pear-shaped cells had inherited nuclei.

Another phenotype presented by the *slt2* mutants is an increased mortality in stationary phase. An example of this sensitivity is shown in Fig. 4. Congenic *slt2-1* and *SLT2*$^+$

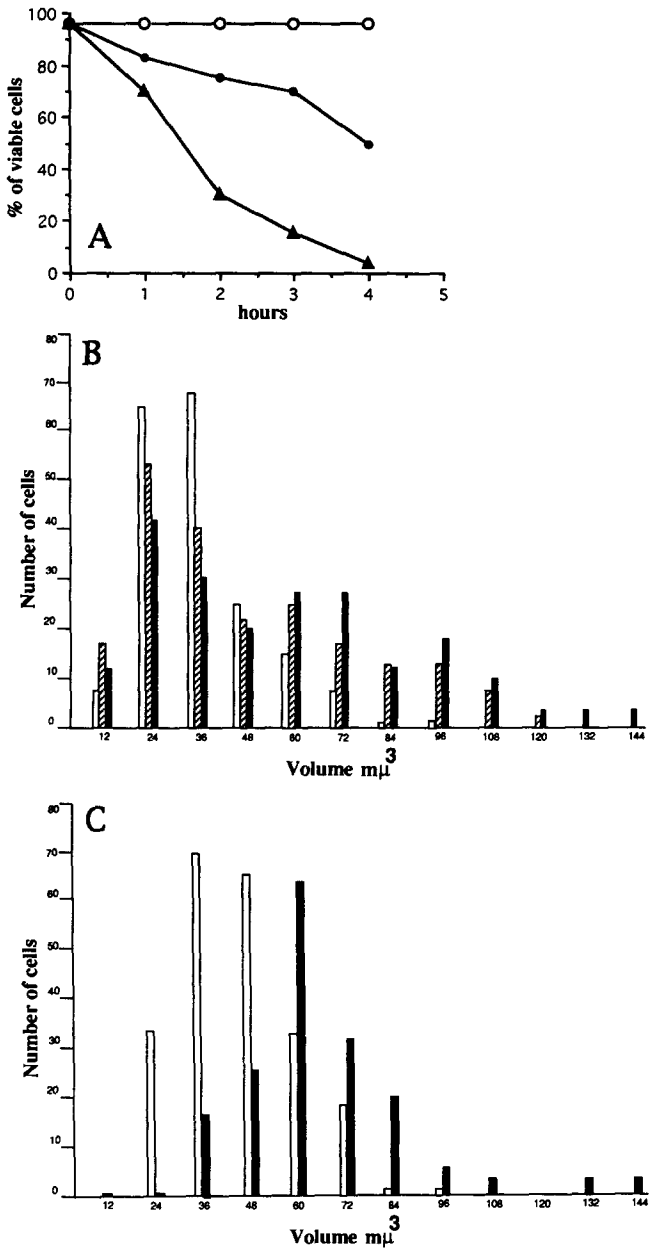

Figure 2. Cell viability and cell size heterogeneity in the *slt2-1* mutant. (*A*) Cell viability of CMY678 *slt2-1* cells growing in exponential phase in YPD at 24°C (○) and after transfer to 30°C (●) or 37°C (▲). Cell viability was determined by spotting cells on YPD plates and observing microscopically the percentage of cells capable of forming a microcolony after 12–24 h of growth at 24°C. (*B*) Histogram of the individual cell volumes of CMY678 *slt2-1* cells grown in exponential phase in YPD at 24°C (□) or after transfer to 30°C for 4 h (▨) or to 37°C for 4 h (■). (*C*) Histogram of the individual cell volumes of the CML6 *SLT2*$^+$ isogenic control strain grown in YPD at 24°C (□) and after transfer to 37°C for 4 h (■). Cells were partitioned into volume classes differing by 12 μm as per Johnston et al. (20).

cells were cultivated in a rich YPD medium at the permissive temperature of 24°C and the cellular viability and budding index were followed over a period of 8 d. The *slt2-1* cells started dying by 3 d of incubation in YPD and only 20% of the mutant cells were viable after 8 d, whereas the *SLT2*$^+$ strain maintained its viability throughout this period of time. *SLT2*$^+$ cells were nearly 100% unbudded from 3 d on in YPD, whereas the mutant cells reached a peak of 84% unbudded cells at 3 d, followed by a drop to 67% unbudded cells at 5 d, before stabilizing at 76% unbudded cells at 8 d of incubation. Cell lysis was visible in the *slt2-1* culture after 3 d of incubation in YPD and a cross-feeding effect may explain the increase in the number of budded cells seen between 3 and 5 d of incubation. However, lysis of both budded and unbudded *slt2* cells in stationary phase suggests that the mutant is not fully capable of mounting a G1 arrest response in addition to its overall starvation sensitivity.

The slt2::HIS3 Disruption Has a Phenotype Similar to That of the slt2-1 Mutant

A disruption of the *SLT2(MPK1)* gene was reported to cause a temperature-sensitive cell lysis defect (25, 60). We repeated this analysis in order to determine whether the same result is true in our strain background and to compare the phenotypes of our EMS-induced *slt2-1* mutant with that of an *SLT2* gene deletion. A 1.3-kb HindIII fragment internal to the *SLT2* gene was replaced with the *HIS3* gene. This substitution deletes sequences encoding all but the first 74 amino acids of Slt2p. The *slt2::HIS3* fragment was used to disrupt one of the *SLT2* genes in a diploid yeast strain. After sporulation and dissection of tetrads at 24°C, two slow growing *slt2::HIS3* segregants and two faster-growing *SLT2*$^+$ segregants were generally observed. The *slt2::HIS3* segregants were temperature sensitive for growth at 37°C with the expected cell-lysis phenotype. We observed that the *slt2::HIS3* strains at 24°C grew more slowly than the *slt2-1* mutant, with *slt2::HIS3* cells showing at 24°C a cell-size heterogeneity and a degree of cell lysis resembling that seen for *slt2-1* at 30°C.

The Heterogeneous Size of the slt2 Mutants Recalls the Phenotype of Actin Cytoskeleton and Polarized Growth Mutants

The presence of both abnormally small and abnormally large cells in the *slt2* cultures could be due to a defect in polarized cell growth. During budding, cell surface growth is directed primarily to the bud via secretory vesicles that are targeted to this portion of the plasma membrane. If this process of directed secretion is partially inhibited without otherwise affecting cell growth and division, then we would expect buds to be smaller than usual and mother cells to grow abnormally large (assuming that untargeted secretory vesicles can fuse with the plasma membrane of the mother cell). Just such a phenotype has been observed for several mutants of the yeast cytoskeleton, including *act1* (34), *myo2* (20), and *tpm1* (29), defective in actin, an unconventional myosin, and tropomyosin, respectively. Because of these similarities, we examined our *slt2* mutants for other phenotypes associated with defects in polarized growth.

Chitin Deposition Is Delocalized in the slt2-1 Mutant

Chitin is deposited in the cell wall to form a ring at the base of the bud in wild-type cells (7). In haploid cells, the site of bud emergence is adjacent to the previous bud, whereas in diploid cells the pattern of budding is bipolar (8). Chitin can

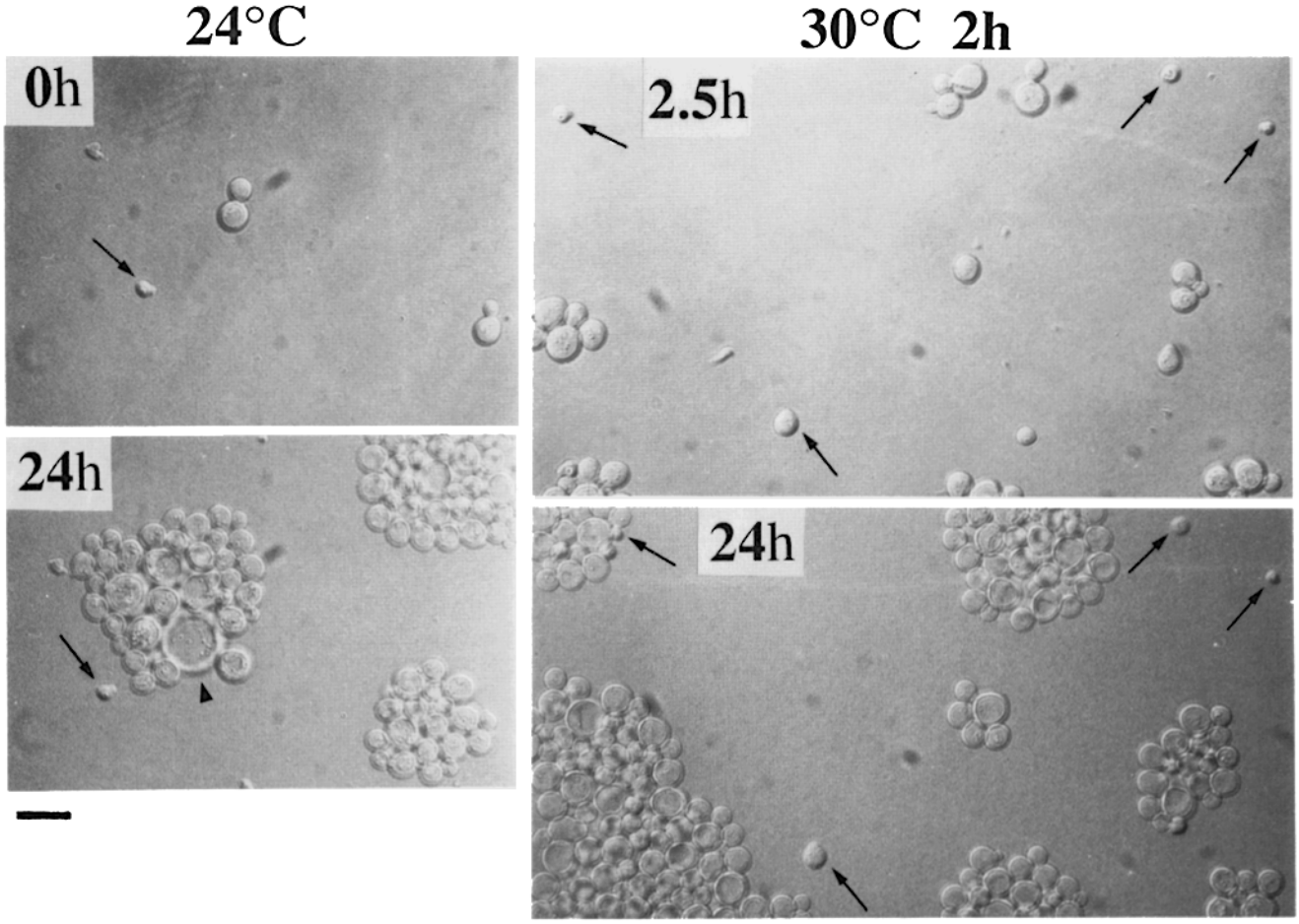

Figure 3. The abnormally small, pear-shaped *slt2-1* cells are stillborn. CMY678 *slt2-1* cells growing at 24°C in YPD, or after a 2-h incubation at 30°C to increase the frequency of the small, pear-shaped cells, were spotted onto a thin layer of YPD agar on a microscope slide and cell proliferation was monitored at room temperature over a 24-h period by time-lapse photomicroscopy. Arrows indicate the positions of the small stillborn cells. Cells of this highly characteristic size and morphology never gave rise to a bud. The arrowhead in the 24°C 24-h panel points to a mother cell that has grown anomalously large. Bar, 10 μm.

be stained specifically with the dye Calcofluor (42, 44). Localization of chitin in the haploid *slt2-1* mutant at the permissive temperature of 24°C (Fig. 5 *A*) was quite similar to that of the wild type (Fig. 5 *E*), with fluorescence restricted to one extremity of the cell in the form of clearly discernible bud scars. After incubation at 37°C for 3 h, wild-type cells showed a slight and transient delocalization of chitin synthesis (Fig. 5 *F*) that we attribute to a transitory G1 arrest induced by the heat shock (Fig. 2 *C* and reference 21). The mutant cells at 37°C showed a much greater chitin delocalization (Fig. 5 *B*). Large, round cells showed the brightest staining with the greatest degree of delocalization. A similar result was seen with the *act1* (34), *myo2* (20), and *tpm1* (29) mutants. We also observed that *slt2/slt2* homozygous diploid mutants have more severe phenotypes than the corresponding *slt2* haploid cells. For example, a heterogeneous cell size

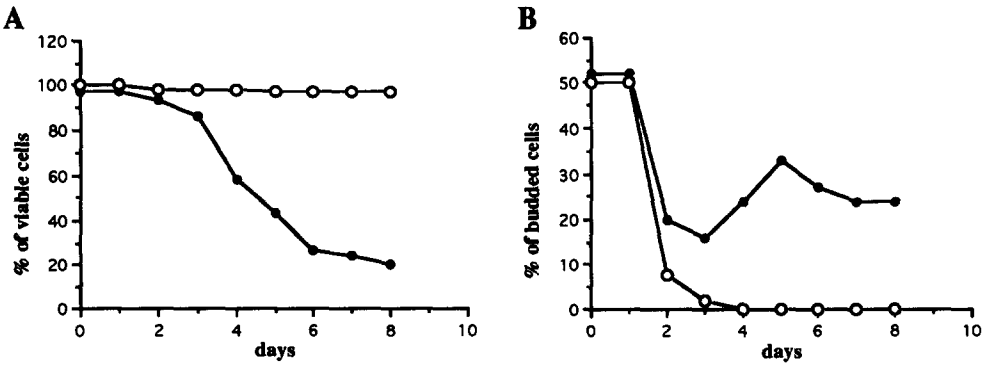

Figure 4. slt2-1 mutants lose viability rapidly in stationary phase. CML12 *slt2-1* (●) and isogenic CML13 *SLT2*$^+$ cells (○) were grown at 24°C in YPD medium over a period of 8 d. Cell viability (*A*) and the percentage of budded cells (*B*) were monitored as a function of time.

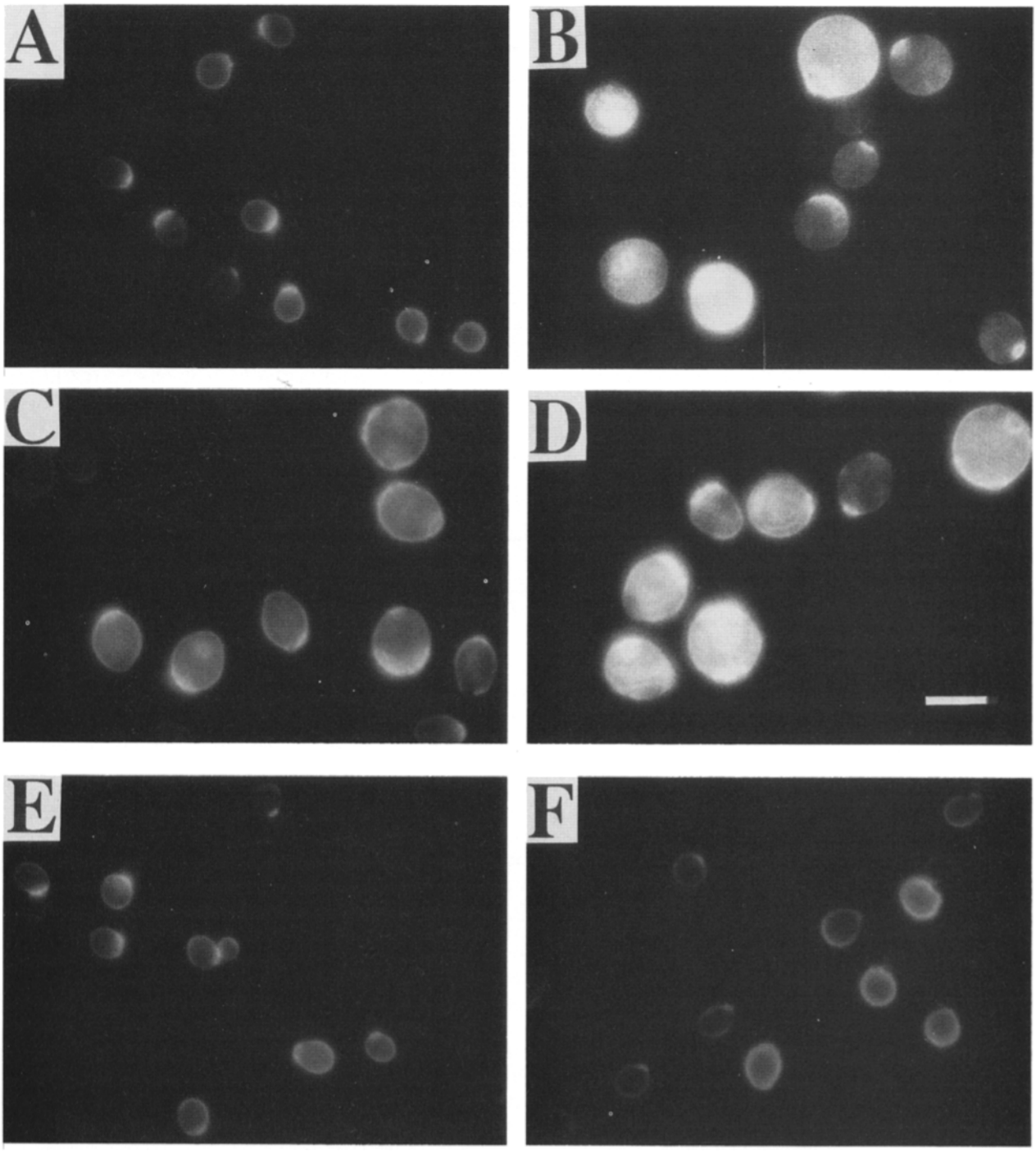

Figure 5. slt2-1 mutants show delocalized deposition of cell surface chitin. *slt2-1* cells growing in YPD were fixed in 3.7% formaldehyde and stained for chitin with Calcofluor. (*A*) CMY678 *slt2-1* haploid cells grown at 24°C and (*B*) after transfer to 37°C for 3 h. (*C*) CML15 *slt2-1* homozygous diploid cells grown at 24°C and (*D*) after transfer to 37°C for 3 h. (*E*) CML6 *SLT2*$^+$ isogenic strain at 24°C and (*F*) after transfer to 37°C for 3 h. All cells are shown at the same magnification. Bar, 10 μm.

and delocalized chitin staining was observed for *slt2-1/slt2-1* diploid cells at the permissive temperature of 24°C (Fig. 5 *C*). The intensity of chitin staining of the *slt2-1/slt2-1* diploid cells increased after incubation at 37°C for 3 h (Fig. 5 *D*). Interestingly, diploid cells deleted for the *TPM1* gene encoding tropomyosin (29) and *myo2-66* homozygous diploids (20) were also reported to have more severe phenotypes than the corresponding haploid cells.

Actin Cortical Patches Are Delocalized in slt2 Mutants

The lysis observed in the *slt2::HIS3* strains at 24°C makes their characterization difficult. The addition of osmotic

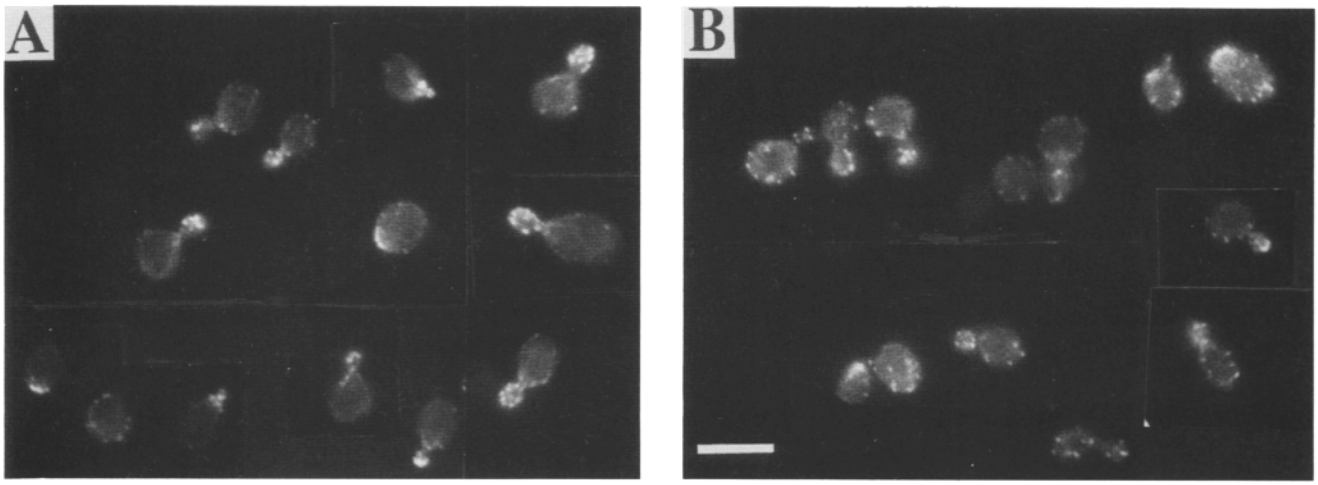

Figure 6. Polarization of cortical actin spots is perturbed in the *slt2::HIS3* mutant. The CML22 *SLT2*$^+$ wild-type (*A*) and the isogenic CML20 *slt2::HIS3* strains (*B*) were grown in YPD + 0.8 M sorbitol at 24°C and then transferred to 37°C for 2 h. Cells were fixed in 3.7% formaldehyde and stained for filamentous actin with rhodamine-conjugated phalloidin. Bar, 10 μm.

stabilizers has been reported to suppress the temperature-sensitive lysis of *slt2(mpk1)* disruption mutants (26, 60). Hence, to overcome the technical difficulties due to cell lysis, we tested the growth of *slt2::HIS3* and *SLT2*$^+$ cells in YPD media containing sorbitol at concentrations of 0.5–1 M. We found 0.8 M sorbitol to give the best suppression of the *slt2::HIS3* mutant phenotypes with the least inhibition of growth of our isogenic *SLT2*$^+$ cells. However, although 0.8 M sorbitol suppressed the temperature sensitivity of the *slt2-1* and *slt2::HIS3* strains, this suppression was incomplete. Some cell lysis and unusually small cells were still observed at 37°C. We looked at the distribution of filamentous actin in *slt2::HIS3* and *SLT2*$^+$ strains at 37°C in YPD + 0.8 M sorbitol using rhodamine-conjugated phalloidin. In *S. cerevisiae*, actin localization reflects the sites of cell surface growth (22).

slt2::HIS3 and wild-type cells growing in YPD medium containing 0.8 M sorbitol at 24°C had a normal actin distribution (data not shown). After transfer to 37°C for 2 h, the *slt2::HIS3* cells growing in YPD medium containing 0.8 M sorbitol showed a clear delocalization in their distribution of cortical actin spots (Fig. 6 *B*) when compared to the *SLT2*$^+$ control strain (Fig. 6 *A*). Numerous actin spots were observed in the mother cell portion of mutant cells with small buds, a situation which is virtually never seen in wild-type cells. There remained a significant residual polarization of the actin spots in buds in these cells that is consistent with the partial suppression of the mutant phenotypes by the sorbitol. Thus, the *SLT2* kinase is required at high temperatures for the normal distribution of the actin cytoskeletal network.

Secretory Vesicles Accumulate in the slt2::HIS3 Mutant

Cytoskeletal mutants with defects in polarized growth, such as *act1* (34), *myo2* (20), and *tpm1* (29), have been shown to accumulate secretory vesicles. We examined *slt2::HIS3* cells growing at 24° or at 37°C in YPD + 0.8 M sorbitol by electron microscopy for a similar phenotype. Sections of glutaraldehyde-fixed cells were postfixed in a 1:1 mixture of 2% osmium tetroxide and 3% potassium ferrocyanide before staining with lead citrate. This treatment results in a strong staining of reducing sugars that allows an excellent visualization of elements of the secretory pathway and the yeast cell wall (Fig. 7). The *slt2::HIS3* cells growing at 24°C in YPD + 0.8 M sorbitol (Fig. 7 *A*) were indistinguishable from wild-type cells. These cells contained a small number of tubules near the inner surface of the plasma membrane or extending from the nuclear membrane and some strongly stained cisternae in the cytoplasm (data not shown). The tubules resemble elements of the endoplasmic reticulum and the cisternae resemble discrete Golgi compartments that have been previously identified by immunoelectron microscopy (41). A small number of secretory vesicles was also observed. In budded cells, the secretory vesicles were found preferentially near the tip of the bud, as shown in Fig. 7 *A* and as seen in wild-type cells (Fig. 7, *WT*). In contrast, two types of aberrant internal morphology were observed in *slt2::HIS3* cells transferred to 37°C for 1.5 h. Both budded and unbudded cells with dramatic accumulations of secretory vesicles distributed throughout the cytoplasm were observed (Fig. 7 *B*).

Figure 7. The *slt2::HIS3* mutant accumulates secretory vesicles and internal cisternal membranes that resemble closely those seen in *act1* and *myo2* mutants. Cells were prepared for electron microscopy as described in Materials and Methods. The cells were grown in YPD + 0.8 M sorbitol whereas the *act1-1* and *myo2-66* cells were grown in YPD without sorbitol. (*A*) A CML20 *slt2::HIS3* cell at 24°C. (*B* and *C*) *slt2::HIS3* cells transferred from 24° to 37°C for 2 h before glutaraldehyde fixation. (*D* and *E*) *myo2-66* cells were transferred from 24° to 37°C for 3 h before fixation. (*F* and *G*) *act1-1* cells were grown at 24°C and then transferred to 37°C for 1.5 h before fixation. *s*, secretory vesicles; *n*, nucleus; *v*, vacuole; *m*, mitochondrion; *g*, Golgi compartments. Bar: (*WT*, *A*, *B*, and *D–G*) 1 μm; (*C*) 0.77 μm.

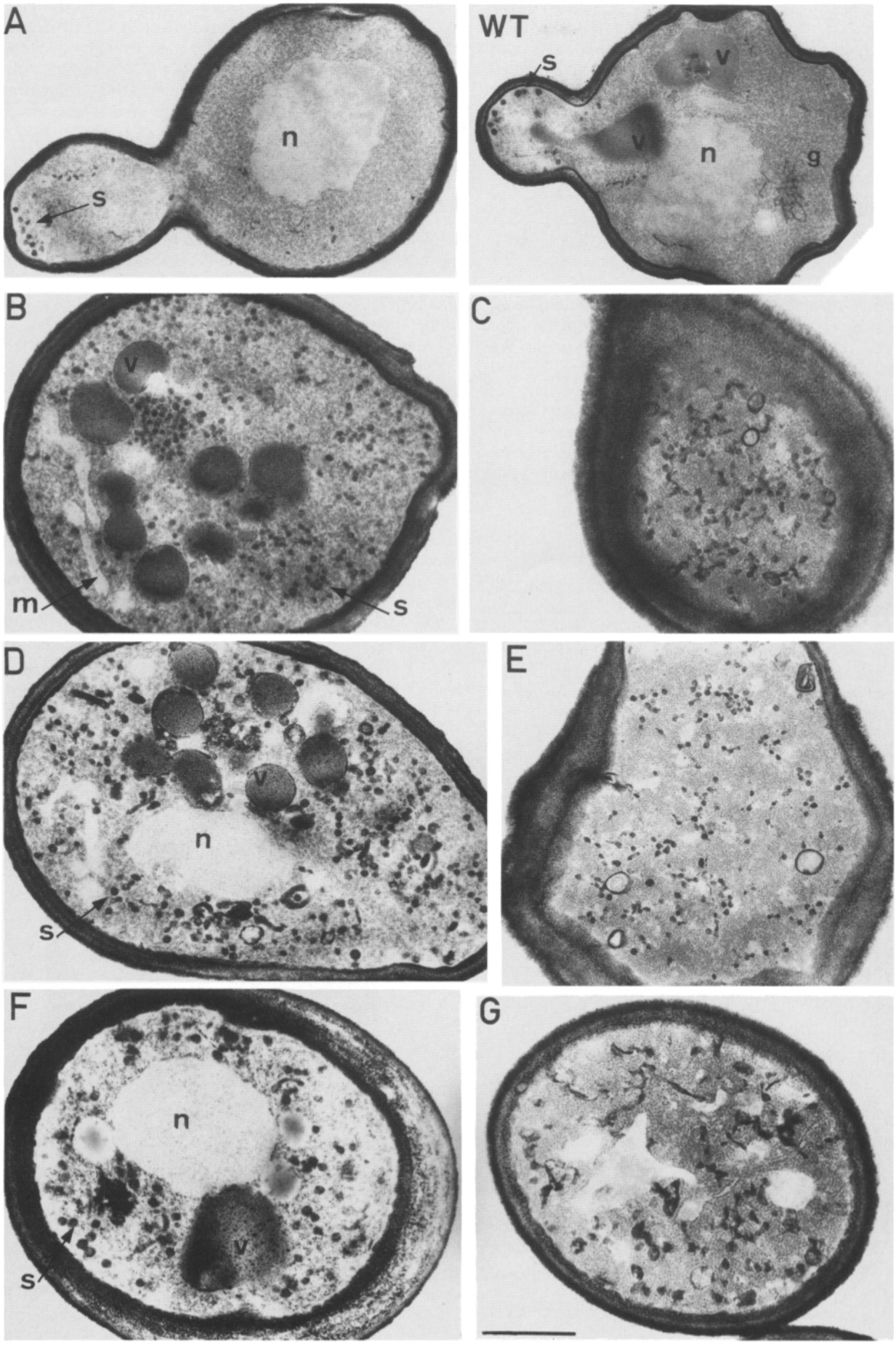
A
n
s
WT
s
v
v
n
g
B
v
m
s
C
D
v
n
s
E
F
n
v
s
G

Fragmented vacuoles were seen in many of these cells. In some sections, a proliferation of tubular networks and unusual doughnut-shaped structures was also observed (Fig. 7 *C*). Similar doughnut-shaped forms have been seen in *sec* mutants blocked late in the secretory pathway (35). Isogenic wild-type cells growing in YPD + 0.8 M sorbitol at 37°C did not show any unusual accumulation of secretory vesicles or internal membranes (Fig. 7, *WT*). We saw no signs of obvious cell wall defects in the *slt2* mutant. A similar analysis was carried out for the *slt2-1* mutant transferred from 24° to 37°C for 1.5 h in YPD without sorbitol. An accumulation of secretory vesicles within the *slt2-1* mutant was also observed, although to a lesser degree than that seen in the *slt2::HIS3* mutant at 37°C.

We have examined thin sections of the *myo2-66* and *act1-1* mutants at the restrictive temperature of 37°C with the same electron microscope stain used to study the *slt2* mutant. We found that the *myo2* (Fig. 7, *D* and *E*) and *act1* (Fig. 7, *F* and *G*) mutants greatly resemble the *slt2* mutant in their accumulation of secretory vesicles and membranous structures. This result is in complete agreement with the previous descriptions of *myo2* (20) and *act1* (36) and suggests that the *slt2* mutant is similarly defective in targeting secretory vesicles to the bud.

Genetic Interactions Implicating SLT2 in Cytoskeletal/Polarized Growth Functions

Characterization of *slt2* mutants reveals defects in polarized growth similar to those seen for the cytoskeletal mutants *act1* and *myo2*. To test for genetic interactions between these mutations, we crossed the *slt2-1* mutant with *act1-1* and *myo2-66* mutants and sporulated the resulting heterozygous diploids. Tetrad analysis showed that the *slt2-1*, *act1-1*, and *myo2-66* single mutant spores germinated and grew well at the permissive temperature of 24°C, whereas the *slt2-1 act1-1* and *slt2-1 myo2-66* double-mutant spores were generally inviable. Approximately 90% of double mutant spores were inviable in a sample of at least 20 tetrads from each cross (the genotype of the dead segregants was deduced from that of the remaining viable spores in each tetrad). The *slt2*, *act1*, and *myo2* mutants are not in isogenic strain backgrounds. We suspect that the existence of a small number of viable double mutants in these crosses to be due to the segregation of polymorphic alleles in the different strain backgrounds that suppress partially the mutant phenotypes. In support of this idea, we found that one-half of the *slt2* segregants in these crosses showed greater residual growth at 37°C than did the *slt2* parental strain. Strain background effects on the severity of cytoskeletal mutant phenotypes have been frequently reported (1, 2, 29).

A more definitive demonstration of colethality between *slt2* and *act1* mutants was obtained by crossing CML29 (*slt2::HIS3*/pFL44-*SLT2*) with CMY776(*act1-1*). The *slt2::HIS3* mutation of strain CML29 is complemented by the *SLT2* gene on the multicopy pFL44(*URA3*) vector (4). Transmission through meiosis of pFL44-*SLT2* occurs with high efficiency. After sporulation and ascus dissection of a CML29 by CMY776 diploid, we analyzed the segregation of the *slt2::HIS3* and the *act1-1* mutations in 10 tetrads in which the pFL44-*SLT2* plasmid was transmitted to all spores. We next examined whether meiotic segregants were able to lose the pFL44-*SLT2* plasmid after non-selective growth on YPD plates at the permissive temperature of 24°C by replica plating to an FOA-containing agar medium at 24°C. FOA (3) inhibits the growth of those cells that contain the pFL44(*URA3*) plasmid. All *slt2::HIS3 act1-1*/pFL44-*SLT2* segregants were incapable of growing on the FOA-containing medium at 24°C, whereas all other segregants grew on this medium. A representative tetratype ascus is shown in Fig. 8. Thus, *slt2::HIS3 act1-1* cells are inviable in the absence of pFL44-*SLT2*. An *slt2::HIS3*/pFL44-*SLT2* strain (CML27) was also crossed to a *myo2-66* mutant (CMY830). All *slt2::HIS3 myo2-66*/pFL44-*SLT2* segregants were unable to grow on FOA plates at 24°C, thereby showing that these two mutations are also incompatible. We conclude that the inactivation of *SLT2* can be lethal in backgrounds in which the actin/Myo2p cytoskeleton is perturbed, thus suggesting a role for the *SLT2* kinase in the optimal functioning of the yeast cytoskeleton.

Deletion of the *SLK1(BCK1)* kinase gene leads to a constellation of mutant phenotypes that greatly resembles those associated with the *slt2* mutants, including a temperature-sensitive cell lysis defect, starvation sensitivity, and heterogeneous cell sizes with a population of unusually small cells (11, 25). We found that the temperature-sensitive growth and lysis phenotype of an *slk1*-Δ2 mutant (11) could be partially suppressed by transforming the strain with a multicopy plasmid containing the *SLT2* kinase. Lee et al. (26) and Irie et al. (19) also observed this suppression and have carried out an extensive series of epistasis experiments suggesting that the Slt2p(Mpk1p) kinase is a downstream activation target of the Slk1p(Bck1p) kinase (see Discussion section).

The *SSD1-v* allele is capable of suppressing a wide range of mutations that were isolated in *ssd1-d* backgrounds (56, 58, 61). Since we knew our lab strains to contain an *ssd1-d* allele (56), and because Costigan et al. had previously shown that *slk1* is suppressed by *SSD1* (11), we tested for suppression of the *slt2-1* mutation by *SSD1-v*. A YCp50-*SSD1-v1* plasmid (58) was capable of partially suppressing the temperature-sensitive growth and lysis of our *slt2-1 ssd1-d* strain. Thus, *SSD1* represents at least one polymorphic allele in dif-

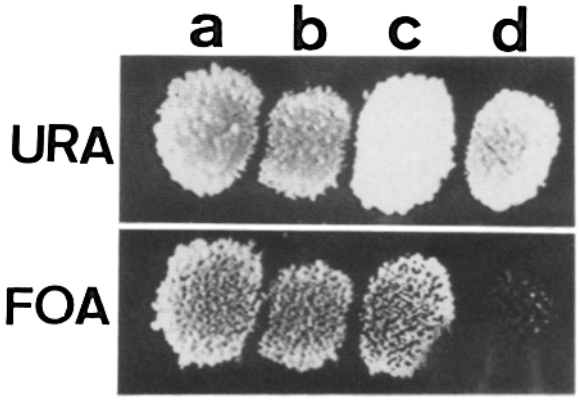

Figure 8. slt2::HIS3 act1-1 double mutants are inviable. The four meiotic segregants resulting from a tetratype ascus obtained after sporulation of the diploid strain CML29 × CMY776 were patched onto a YPD plate at 24°C. The spore genotypes are: (*a*) *act1-1 SLT2*/pFL44-*SLT2*; (*b*) *ACT1 SLT2*/pFL44-*SLT2*; (*c*) *ACT1 slt2::HIS3*/pFL44-*SLT2*; and (*d*) *act1-1 slt2::HIS3*/pFL44-*SLT2*. The cells were then replica plated to a synthetic medium without uracil (*URA*) or to an FOA-containing medium (*FOA*) at the 24°C permissive temperature for both mutants.

ferent laboratory strain backgrounds that can modify the penetrance of the *slt2* phenotypes. Ssdlp (also known as Srklp) has been suggested to play a role in protein phosphatase function, but no biochemical studies of this protein have yet been reported (58, 61).

Discussion

slt2 Mutants Have Phenotypes Reminiscent of Actin Cytoskeletal Mutants and Are Defective in Polarized Growth

slt2 mutants exhibit a number of phenotypes that recall those of yeast cytoskeletal mutants, including cell-size heterogeneity and morphological defects, delocalization of both chitin deposition and actin cortical spots, and the accumulation of secretory vesicles. Similar phenotypes have been reported for mutants of actin (*act1*) (34), an unconventional myosin (*myo2*) (20), tropomyosin (*tpm1*) (29), and *sac1*, *sac2*, and *sac3* (cold-sensitive suppressors of an actin mutant) (36). These phenotypes may all be manifestations of defects in polarized growth in these mutants due to perturbations of the actin cytoskeleton. Hence, the actin cytoskeleton seems to be required for directing secretory growth to the chosen site of bud emergence in unbudded cells, and then, for restricting growth to the bud after bud emergence. If this process is disturbed, then secretory vesicles (and possibly Golgi compartments as well) (41) will not be efficiently targeted to the bud, and the buds will be smaller than usual. If the non-targeted secretory vesicles can fuse to the plasma membrane of mother cells, then these cells should grow abnormally large at the expense of the buds. The fact that some cytoskeletal mutant cells do get larger and show a delocalized deposition of chitin in their cell walls indicates that secretory vesicles can fuse to the mother cell plasma membrane. However, the observation that secretory vesicles and aberrant cisternal membranes accumulate within the *act1*, *myo2*, and *slt2* mutants suggests that the nontargeted secretory vesicles do not fuse efficiently to the cell membrane.

Cell size heterogeneity accompanied by abnormal actin distributions and delocalized chitin deposition has also been observed in profilin (*pfy*) (17), fimbrin (*sac6*) (1), actin capping protein (*cap1* and *cap2*) (2), *rho3* and *rho4* (33), and *bem1* (10) mutants. These mutants have not yet been examined by electron microscopy for accumulation of secretory vesicles. Profilin, fimbrin, and actin capping protein all interact directly with actin, but the relationship of Rho3p, Rho4p, and Bem1p with the actin cytoskeleton has not yet been determined. The similarity of the *slt2* and cytoskeleton mutant phenotypes suggests that the *SLT2* kinase phosphorylates one or more of the cytoskeletal components and/or the bud-site complex proteins in such a way that polarized growth is stimulated. Less direct mechanisms are also possible. The *SLK1(BCK1)* kinase is a putative upstream activator of the *SLT2(MPK1)* kinase (see below). Costigan et al. have shown that *slk1 spa2* double mutants are inviable, whereas either single mutant is viable at 24°C (11). Since Spa2p is specifically localized to sites of polarized growth (53), this synthetic lethal interaction supports the idea that *SLK1/SLT2* pathway functions in regulating polarized growth.

The starvation sensitivity of the *slt2* mutants (Fig. 4) is one phenotype that has not been reported for the cytoskeletal mutants. It is not clear whether the necessity of *SLT2* for normal stationary phase viability is related to its postulated role in the actin cytoskeleton and cell polarity, or whether it represents a completely independent function of the kinase. The *slk1* mutant also loses viability rapidly upon nutrient starvation (11).

Deletion of the *SLT2* gene is not lethal. The *slt2::HIS3* cells grow slowly at 24°C, have defects in cell polarity, and are prone to lysis. At 37°C, cells die rapidly with lots of lysis. Many cytoskeletal components have similarly been shown to be necessary for normal cell polarity and cytoskeletal structure at 22°–30°C without being necessary for cell viability at these temperatures. Most of these proteins, including fimbrin (1), profilin (17), tropomyosin (29), Sac1p (36), Sac7p (14), and Bem1p (10) are required for viability at low (14°–16°C) and/or high (36°–38°C) temperatures. The relative dispensibility of these proteins may mean that there are functionally redundant equivalents still to be found within the cell. Alternatively, it may mean that the actin cytoskeleton can function, albeit poorly, in the absence of these proteins at 22°–30°C, but not under conditions of stress, such as growth at low or high temperatures.

Torres et al. (60) have suggested that *SLT2* is involved in cell wall biosynthesis. This suggestion was based largely on the fact that osmotic stabilizers can suppress (partially in our strain background) the temperature-sensitive cell lysis phenotype of *slt2* mutants. However, mutants of the cortical cytoskeleton in yeast (1, 34) and in animal cells (30) can be fragile and prone to lysis. As discussed by Costigan et al. (11), mutants with defective cytoskeletons can sometimes be suppressed by osmotic stabilizers. It is also possible that osmotic stabilizers suppress *slt2* phenotypes by a completely distinct mechanism. Slt2p is clearly a member of the MAP kinase family (see Fig. 1 and reference 26). Recently, another MAP kinase isoform in *S. cerevisiae*, Hog1p, was shown to be necessary for cell growth in media of high osmolarity (5). Hog1p is tyrosine phosphorylated, and presumably activated, upon addition of 0.7 M sorbitol to the growth medium. Given the extensive sequence similarity between Slt2p and Hog1p (see Fig. 1), it is conceivable that the partial suppression of *slt2* phenotypes could occur by Hog1p activation allowing it to phosphorylate some of the substrates that are normally phosphorylated by Slt2p. In summary, suppression of *slt2* cell lysis by osmotic agents may be explained in several different ways. We suggest that any cell wall defects that exist in *slt2* mutants could be secondary consequences of defects in polarized growth.

Two other MAP kinase isoforms of *S. cerevisiae*, FUS3 and KSS1, are activated by the mating pheromone pathway (16). We have observed that *slt2* mutants are slightly defective in projection formation upon addition of alpha factor or in mating mixtures of yeast cells (data not shown). *slk1(bck1)* mutants also exhibit a projection formation defect (11). The formation of a mating projection is another manifestation of polarized cell growth in the yeast life cycle. The fact that *slt2* mutants are only slightly defective in projection formation may be due to the activation of the *FUS3* and *KSS1* kinases allowing them to phosphorylate and activate substrates critical for polarized growth that are normally activated by the *SLT2* kinase during mitotic growth.

Activation of the SLT2(MPK1) MAP Kinase Homolog

Recent genetic evidence of Lee et al. (26) and Irie et al. (19) suggests that the *SLT2(MPK1)* kinase is activated in a cascade in which the *BCK1(SLK1)* kinase activates the redundant pair of kinases *MKK1* and *MKK2*, which in turn activate the *SLT2(MPK1)* kinase. Remarkably, the *MKK* kinases are most similar in sequence to a class of MAP kinase-kinases including *STE7*, *PBS2*, *byr1*$^+$, and MAPKK (15). Furthermore, Bck1p(Slk1p) is most similar in its kinase catalytic domain to the *STE11* kinase which is thought to phosphorylate and activate the *STE7* MAPKK. A dominant, activated mutant of the *BCK1(SLK1)* gene has been isolated as a bypass suppressor of protein kinase C mutants (*pkc1*). It was thus proposed that Pkc1p is an activator of the Bck1p(Slk1p)-Mkk1p/2p-Slt2p(Mpk1p) cascade. *pkc1* mutants have an osmotic-remedial cell lysis phenotype that has been suggested to be due to cell wall defects (27, 38).

We isolated our *slt2* allele in a screen for mutants that enhance the division defect of partially inactivated *cdc28* mutants. This phenotypic enhancement seems to concern a G1-specific function of Cdc28p, since it was observed with the *cdc28-4* allele that is mainly defective in G1 functions of Cdc28p, and it was not seen with the *cdc28-1N* allele that is mainly defective in G2/mitotic functions of Cdc28p. Our phenotypic analysis has suggested that Slt2p promotes polarization of cell growth to the bud. Cdc28p activation at Start in G1-phase also promotes bud emergence. We thus propose that the *SLT2* pathway is either a downstream activation target of the *CDC28* kinase or that Slt2p and Cdc28p function in parallel in promoting bud emergence and subsequent growth. A *Xenopus* 42-kD MAP kinase can be activated by the addition of CDC2-MPF to interphase oocyte extracts. CDC2-MPF functions upstream of a MAPKK kinase in this system (24). 42- and 44-kD MAP kinases are also activated biphasically in the G1/S and G2/M phases of Chinese hamster ovary cells (59). Ultimately, direct biochemical assays will determine whether Slt2p(Mpk1p) activation is dependent on Cdc28p and/or Pkc1p and whether its activation varies during the cell division cycle.

We thank Corinne Le Moal for technical assistance in preparing specimens for electron microscopy and we thank Christine Costigan and Mike Snyder for strains and discussions. Thanks as well to John Cooper, Mike Gustin and John Pringle for discussions and to Catherine Jackson for reviewing the manuscript.

Cristina Mazzoni was supported by a fellowship from the Istituto Pasteur Fondazione Cenci Bolognetti in Italy and Patrick Zarzov by a fellowship from the French Ministère de la Recherche et de l'Espace.

Received for publication 14 March 1993 and in revised form 19 October 1993.

References

1. Adams, A. E. M., D. Botstein, and D. G. Drubin. 1991. Requirement of yeast fimbrin for actin organization and morphogenesis *in vivo*. *Nature* 354:404–408.
2. Amatruda, J. F., D. J. Gattermeir, T. S. Karpova, and J. A. Cooper. 1992. Effects of null mutations and overexpression of capping protein on morphogenesis, actin distribution and polarized secretion in yeast. *J. Cell Biol.* 119:1151–1162.
3. Boeke, J. D., F. Lacroute, and G. R. Fink. 1984. A positive selection for mutants lacking orotidine-5'-phosphate decarboxylase activity in yeast: 5-fluoro-orotic acid resistance. *Mol. Gen. Genet.* 197:345–346.
4. Bonneaud, N., O. Ozier-Kalogeropoulos, G. Li, M. Labouesse, L. Minvielle-Sebastia, and F. Lacroute. 1991. A family of low and high copy replicative, Integrative and single-stranded *S. cerevisiae/E. coli* shuttle vectors. *Yeast.* 7:609–615.
5. Brewster, J. L., T. de Valoir, N. D. Dwyer, E. Winter, and M. C. Gustin. 1993. An osmosensing signal transduction pathway in yeast. *Science (Wash. DC).* 259:1760–1763.
6. Brockerhoff, S. E., and T. N. Davis. 1992. Calmodulin Concentrates at Regions of Cell Growth in *Saccharomyces cerevisiae*. *J. Cell Biol.* 118:619–629.
7. Cabib, E., R. Roberts, and B. Bowers. 1982. Synthesis of the yeast cell wall and its regulation. *Annu. Rev. Biochem.* 51:763–793.
8. Chant, J., and I. Herskowitz. 1991. Genetic control of bud site selection in yeast by a set of gene products that constitute a morphogenetic pathway. *Cell.* 65:1203–1212.
9. Chant, J., and J. R. Pringle. 1991. Budding and cell polarity in *Saccharomyces cerevisiae*. *Curr. Opin. Genet. Dev.* 1:342–350.
10. Chenevert, J., K. Corrado, A. Bender, J. Pringle, and I. Herskowitz. 1992. A yeast gene (*BEM1*) necessary for cell polarization whose product contains two SH3 domains. *Nature (Lond.).* 356:77–79.
11. Costigan, C., S. Gehrung, and M. Snyder. 1992. A synthetic lethal screen identifies *SLK1*, a novel protein kinase homolog implicated in yeast cell morphogenesis and cell growth. *Mol. Cell. Biol.* 12:1162–1178.
12. Drubin, D. G. 1991. Development of cell polarity in budding yeast. *Cell.* 65:1093–1096.
13. Ducommun, B., P. Brambilla, M.-A. Félix, B. R. Franza Jr., E. Karsenti, and G. Draetta. 1991. cdc2 phosphorylation is required for its interaction with cyclin. *EMBO (Eur. Mol. Biol. Organ.) J.* 10:3311–3319.
14. Dunn, T. M., and D. Shortle. 1990. Null alleles of *SAC7* suppress temperature-sensitive actin mutations in *Saccharomyces cerevisiae*. *Mol. Cell. Biol.* 10:2308–2314.
15. Errede, B., and D. E. Levin. 1993. A conserved kinase cascade for MAP kinase activation in yeast. *Curr. Opin. Cell Biol.* 5:254–260.
16. Gartner, A., K. Nasmyth, and G. Ammerer. 1992. Signal transduction in *Saccharomyces cerevisiae* requires tyrosine and threonine phosphorylation of FUS3 and KSS1. *Genes & Dev.* 6:1280–1292.
17. Haarer, B. K., S. H. Lillie, A. E. M. Adams, V. Magdolen, W. Bandlow, and S. S. Brown. 1990. Purification of profilin from *Saccharomyces cerevisiae* and analysis of profilin-deficient cells. *J. Cell Biol.* 110:105–114.
18. Hartwell, L. H., J. Culotti, J. R. Pringle, and B. J. Reid. 1974. Genetic control of the cell division cycle in yeast. *Science (Wash. DC).* 183: 46–51.
19. Irie, K., M. Takase, K. S. Lee, D. E. Levin, H. Araki, K. Matsumoto, and Y. Oshima. 1993. *MKK1* and *MKK2*, which encode *Saccharomyces cerevisiae* mitogen-activated protein kinase-kinase homologs, function in the pathway mediated by protein kinase C. *Mol. Cell. Biol.* 13:3076–3083.
20. Johnston, G. C., J. A. Prendergast, and R. A. Singer. 1991. The *Saccharomyces cerevisiae MYO2* gene encodes an essential myosin for vectorial transport of vesicles. *J. Cell Biol.* 113:539–551.
21. Johnston, G. C., and R. A. Singer. 1980. Ribosomal precursor RNA metabolism and cell division in the yeast *Saccharomyces cerevisiae*. *Mol. Gen. Genet.* 178:357–360.
22. Kilmartin, J. V., and A. E. M. Adams. 1984. Structural rearrangements of tubulin and actin during the cell cycle of the yeast *Saccharomyces*. *J. Cell Biol.* 98:922–933.
23. Kim, H. B., B. K. Haarer, and J. R. Pringle. 1991. Cellular morphogenesis in the *Saccharomyces cerevisiae* cell cycle: localization of the *CDC3* gene product and the timing of events at the budding site. *J. Cell Biol.* 112: 535–544.
24. Kosako, H., E. Nishida, and Y. Gotoh. 1993. cDNA cloning of MAP kinase kinase reveals kinase cascade pathways in yeasts to vertebrates. *EMBO (Eur. Mol. Biol. Organ.) J.* 12:787–794.
25. Lee, K. S., and D. E. Levin. 1992. Dominant mutations in a gene encoding a putative protein kinase (*BCK1*) bypass the requirement for a *Saccharomyces cerevisiae* protein kinase C homolog. *Mol. Cell. Biol.* 12:172–182.
26. Lee, K. S., K. Irie, Y. Gotoh, Y. Watanabe, H. Araki, E. Nishida, K. Matsumoto, and D. E. Levin. 1993. A yeast mitogen-activated protein kinase homolog (Mpk1p) mediates signalling by protein kinase C. *Mol. Cell. Biol.* 13:3067–3075.
27. Levin, D. E., and E. Bartlett-Heubusch. 1992. Mutants in the *S. cerevisiae PKC1* gene display a cell cycle-specific osmotic stability defect. *J. Cell Biol.* 116:1221–1229.
28. Lew, D. J., and S. I. Reed. 1993. Morphogenesis in the yeast cell cycle: regulation by Cdc28 and cyclins. *J. Cell Biol.* 120:1305–1320.
29. Liu, H., and A. Bretscher. 1992. Characterization of *TPM1* disrupted yeast cells indicates an involvement of tropomyosin in directed vesicular transport. *J. Cell Biol.* 118:285–299.
30. Luna, E. J., and A. L. Hitt. 1992. Cytoskeleton-plasma membrane interactions. *Science (Wash. DC).* 258:955–964.
31. Madden, K., and M. Snyder. 1992. Specification of sites for polarized growth in *Saccharomyces cerevisiae* and the influence of external factors on site selection. *Mol. Biol. Cell.* 3:1025–1035.
32. Madden, K., C. Costigan, and M. Snyder. 1992. Cell polarity and morphogenesis in *Saccharomyces cerevisiae*. *Trends Cell Biol.* 2:22–29.
33. Matsui, Y., and A. Toh-e. 1992. Yeast *RHO3* and *RHO4 ras* superfamily genes are necessary for bud growth, and their defect is suppressed by a

high dose of bud formation genes *CDC42* and *BEM1*. *Mol. Cell. Biol.* 12:5690–5699.
34. Novick, P., and D. Botstein. 1985. Phenotypic analysis of temperature-sensitive yeast actin mutants. *Cell.* 40:405–416.
35. Novick, P., S. Ferro, and R. Schekman. 1981. Order of events in the yeast secretory pathway. *Cell.* 25:461–469.
36. Novick, P., B. C. Osmond, and D. Botstein. 1989. Suppressors of yeast actin mutants. *Genetics.* 121:659–674.
37. Nurse, P. 1990. Universal control mechanism regulating onset of M-phase. *Nature (Lond.).* 344:503–508.
38. Paravicini, G., M. Cooper, L. Friedli, D. J. Smith, J.-L. Carpentier, L. S. Klig, and M. A. Payton. 1992. The osmotic integrity of the yeast cell requires a functional *PKC1* gene product. *Mol. Cell. Biol.* 12:4896–4905.
39. Pelech, S. L., and J. S. Sanghera. 1992. Mitogen-activated protein kinases: versatile transducers for cell signaling. *Trends Biochem. Sci.* 17:233–238.
40. Piggott, J. R., R. Rai, and B. L. A. Carter. 1982. A bifunctional gene product involved in two phases of the yeast cell cycle. *Nature (Lond.).* 298:391–393.
41. Preuss, D., J. Mulholland, A. Franzusoff, N. Segev, and D. Botstein. 1992. Characterization of the *Saccharomyces* golgi complex through the cell cycle by immunoelectron microscopy. *Mol. Biol. Cell* 3:789–803.
42. Pringle, J. R., R. A. Preston, A. E. M. Adams, T. Stearns, D. G. Drubin, B. K. Haarer, and E. W. Jones. 1989. Fluorescence microscopy methods for yeast. *Meth. Cell Biol.* 31:357–434.
43. Pringle, J. R., and L. H. Hartwell. 1981. The *Saccharomyces cerevisiae* Cell Cycle. Vol. 1. J. N. Strathern, E. W. Jones, and J. R. Broach, editors. Cold Spring Harbor Laboratory, Cold Spring Harbor, NY. 97–142.
44. Pringle, J. R., A. E. M. Adams, D. G. Drubin, and B. K. Haarer. 1991. Immunofluorescence methods for yeast. *Methods Enzymol.* 194:565–602.
45. Reed, S. I. 1992. The role of p34 kinases in the G1 to S-phase transition. *Annu. Rev. Cell Biol.* 8:529–561.
46. Reed, S. I., and C. Wittenberg. 1990. Mitotic role for the Cdc28 protein kinase of *Saccharomyces cerevisiae*. *Proc. Natl. Acad. Sci. USA.* 87: 5697–5701.
47. Rose, M. D., P. Novick, J. H. Thomas, D. Botstein, and G. R. Fink. 1987. A *Saccharomyces cerevisiae* genomic plasmid bank based on a centromere-containing shuttle vector. *Gene.* 60:237–243.
48. Rothstein, R. J. 1983. One-step gene disruption in yeast. *Methods Enzymol.* 101:202–211.
49. Sambrook, J., E. F. Fritsch, and T. Maniatis. 1989. Molecular cloning: a laboratory manual, 2nd edition. Cold Spring Harbor Laboratory, Cold Spring Harbor, NY.
50. Sherman, F. 1991. Getting started with yeast. *Meth. Enzymol.* 194:3–21.
51. Sikorski, R. S., and P. Hieter. 1989. A System of shuttle vectors and yeast host strains designed for efficient manipulation of DNA in *Saccharomyces cerevisiae*. *Genetics.* 122:19–27.
52. Simon, M. A., D. L. Bowtell, G. S. Dodson, T. R. Laverty, and G. M. Rubin. 1991. Ras1 and a putative guanine nucleotide exchange factor perform crucial steps in signaling by the sevenless protein tyrosine kinase. *Cell.* 67:701–716.
53. Snyder, M. 1989. The *SPA2* protein of yeast localizes to sites of cell growth. *J. Cell Biol.* 108:1419–1429.
54. Snyder, M., S. Gehrung, and B. D. Page. 1991. Studies concerning the temporal and genetic control of cell polarity in *Saccharomyces cerevisiae*. *J. Cell Biol.* 114:515–532.
55. Staebell, M., and D. R. Soll. 1985. Temporal and spatial differences in cell wall expansion during bud and mycelium formation in *Candida albicans*. *J. Gen. Microbiol.* 131:1467–1480.
56. Stettler, S., N. Chiannilkulchai, S. Hermann-Le Denmat, D. Lalo, F. Lacroute, A. Sentenac, and P. Thuriaux. 1993. A general suppressor of RNA polymerase I, II and III mutations in *Saccharomyces cerevisiae*. *Mol. Gen. Genet.* 239:169–176.
57. Surana, U., H. Robitsch, C. Price, T. Schuster, I. Fitch, A. B. Futcher, and K. Nasmyth. 1991. The role of CDC28 and cyclins during mitosis in the budding yeast *S. cerevisiae*. *Cell.* 65:145–161.
58. Sutton, A., D. Immanuel, and K. T. Arndt. 1991. The *SIT4* protein phosphatase functions in late G1 for progression into S phase. *Mol. Cell. Biol.* 11:2133–2148.
59. Tamemoto, H., T. Kadowaki, K. Tobe, K. Ueki, T. Izume, Y. Chatani, M. Kohno, M. Kasuga, Y. Yazaki, and Y. Akanuma. 1992. Biphasic activation of two mitogen-activated protein kinases during the cell cycle in mammalian cells. *J. Biol. Chem.* 267:20293–20297.
60. Torres, L., H. Martin, M. I. Garcia-Saez, J. Arroyo, M. Molina, M. Sanchez, and C. Nombela. 1991. A protein kinase gene complements the lytic phenotype of *Saccharomyces cerevisiae lyt2* mutants. *Mol. Microbiol.* 5:2845–2854.
61. Wilson, R. B., A. A. Brenner, T. B. White, M. J. Engler, J. P. Gaughran, and K. Tatchell. 1991. The *Saccharomyces cerevisiae SRK1* Gene, a suppressor of *bcy1* and *ins1*, may be involved in protein phosphatase function. *Mol. Cell. Biol.* 11:3369–3373.